

# Group Equivariant BEV for 3D Object Detection

1<sup>st</sup> Hongwei Liu

*Fujian Institute of Research on  
the Structure of Matter  
Chinese Academy of Sciences  
Fuzhou, China  
hwhongwei.liu@foxmail.com*

2<sup>nd</sup> Jian Yang\*

*School of Geospatial Information  
Information Engineering University  
Zhengzhou, China  
jian.yang@tum.de*

3<sup>rd</sup> Jianfeng Zhang

*Fujian Institute of Research on  
the Structure of Matter  
Chinese Academy of Sciences  
Fuzhou, China  
zhangjf@fjirsm.ac.cn*

4<sup>th</sup> Dongheng Shao

*Fujian Institute of Research on  
the Structure of Matter  
Chinese Academy of Sciences  
Fuzhou, China  
shaodongheng@fjirsm.ac.cn*

5<sup>th</sup> Jielong Guo

*Fujian Institute of Research on  
the Structure of Matter  
Chinese Academy of Sciences  
Fuzhou, China  
gjl@fjirsm.ac.cn*

6<sup>th</sup> Shaobo Li

*School of Electrical Engineer  
and Automation  
Xiamen University of Technology  
Xiamen, China  
lishaobogo@gmail.com*

7<sup>th</sup> Xuan Tang

*Fujian Institute of Research on  
the Structure of Matter  
Chinese Academy of Sciences  
Fuzhou, China  
xtang@cee.ecnu.edu.cn*

8<sup>th</sup> Xian Wei

*Fujian Institute of Research on  
the Structure of Matter  
Chinese Academy of Sciences  
Fuzhou, China  
xian.wei@tum.de*

**Abstract**—Recently, 3D object detection has attracted significant attention and achieved continuous improvement in real road scenarios. The environmental information is collected from a single sensor or multi-sensor fusion to detect interested objects. However, most of the current 3D object detection approaches focus on developing advanced network architectures to improve the detection precision of the object rather than considering the dynamic driving scenes, where data collected from sensors equipped in the vehicle contain various perturbation features. As a result, existing work cannot still tackle the perturbation issue. In order to solve this problem, we propose a group equivariant bird’s eye view network (GeqBevNet) based on the group equivariant theory, which introduces the concept of group equivariant into the BEV fusion object detection network. The group equivariant network is embedded into the fused BEV feature map to facilitate the BEV-level rotational equivariant feature extraction, thus leading to lower average orientation error. In order to demonstrate the effectiveness of the GeqBevNet, the network is verified on the nuScenes validation dataset in which mAOE can be decreased to 0.325. Experimental results demonstrate that GeqBevNet can extract more rotational equivariant features in the 3D object detection of the actual road scene and improve the performance of object orientation prediction.

## I. INTRODUCTION

As one of the critical components of self-driving cars [1] and autonomous mobile robots [2], perception systems have witnessed continuous development in recent years. In order to

guarantee an application-ready performance of environmental perception, perception systems often employ various sensors to obtain environmental information. For example, LiDAR uses the optical time-of-flight(TOF) method to obtain point clouds with distance and geometric information through laser beams, which provide outlines and position information of its surrounding objects. However, several defects still limit LiDAR’s further applications, such as the high cost, sparse point clouds of distant objects, and lack of semantics. Compared with LiDAR, cameras have been widely used in perception systems [6], [7] in real-world applications, with mature technology and low cost. It can provide rich semantic information, such as the color and texture of objects, and it can also recognize traffic lights and signboards in outdoor scenes. However, many uncertainties remain under extreme driving conditions, e.g., rainy, snowy, and too-bright weather conditions. It is difficult to extract sufficient context information [8] from dim or too-bright images. Therefore, multi-sensor fusion techniques are favored, which can safely and efficiently perform environment perception tasks.

Extensive research has recently investigated object detection networks based on multi-sensor fusion. The multi-modal information provided by multi-sensors can effectively utilize the advantages of each sensor to provide safe and reliable perception information [10], [11], [12], [13]. However, most of these sensor fusion research chose one sensor as the dominant data source while using the other sensor for supplementary information. For example, the work in [10] used camera inputs to acquire the image features from the front view while

This research is supported by National Natural Science Foundation of China (No.42130112) and KartoBit Research Network(No.KRN2201CA). Partially supported by ‘Fujian Science & Technology Innovation Laboratory for Optoelectronic Information of China’ (No.2021ZZ120).

\*Corresponding Author

projecting the point cloud into the front view for sensor fusion. This approach makes little use of the geometric features of the point cloud. The other work [11] explored the geometric features in the LiDAR point clouds, then attached the semantic features of the images to the point clouds to perform object detection on the point clouds, which discards the semantic density in the images. Unifying sensory inputs from cameras and LiDAR in the same form for data fusion have become an important research topic of multi-sensor fusion. Recently, two important research work [14], [15] have contributed to such effort and employ a bird’s eye view (BEV) for feature fusion. The BEV framework has enabled a unified top-down representation of sensory inputs from different modalities and alleviates the issue of object occlusion.

The BEV-based fusion methods overcome the shortcomings of previous fusion methods that cannot leverage both semantic and geometric information, thus resulting in a better performance in object detection. However, they have not considered the sensory perturbation of moving objects and the varying road scenes. Detecting moving objects with various perturbation characteristics is a non-trivial task that has not been well studied, especially in developing advanced neural network architectures robust to varying perturbation. Data augmentation is an alternative method to improve the detection performance for moving objects, but it relies on sufficient training data and requires large computational overhead. In contrast to data augmentation, another work [3] used group equivariant methods to solve the data redundancy problem of data augmentation, in addition to alleviating the performance degradation caused by vehicle rotation, which is a highly worthwhile idea.

To address the above issues, we propose a group equivariant BEV object detection network named group equivariant bird’s eye view network (**GeqBevNet**). A group equivariant network is embedded into a 3D detection framework to extract rotational equivariant features. Specifically, the camera BEV generation network and the LiDAR BEV generation network generate two BEV-based sensory input representations separately and fuse these two BEVs. Furthermore, the group equivariant network is embedded after the fused BEV and extracts the rotational equivariant features using group operations. We achieve excellent experimental results on the challenging benchmark dataset nuScenes [17] for autonomous driving. On the NuScenes validation set, GeqBevNet achieves 62.2% on mean Average Precision (mAP) and 0.325 on mean Average Orientation Error (mAOE). Compared with other advanced networks, GeqBevNet has a significantly lower mAOE. It shows that our GeqBevNet performs orientation prediction better in scene rotation. The main contributions of this paper are as follows:

- We construct an embeddable group equivariant network based on group equivariant theory to extract rotational equivariant features at BEV-level.
- To satisfied the requirement of embeddability, the group equivariant network can be freely and reasonably embedded into the object detection network.

- To demonstrate the effectiveness of the proposed GeqBevNet, we conducted extensive experiments on the nuScenes dataset, where we achieved better results compared to advanced object detection networks.

## II. RELATED WORK

### A. 3D Object Detection

1) *Camera-based 3D Object Detection*: 3D object detection directly on the front view is still a challenge. In the previous camera-based 3D object detection methods, one approach uses mature 2D object detection methods to extract region proposals on the front view, then return to 3D bounding boxes. Chen et al. [18] generated a set of 2D object region proposals from a single image and then used the proposed method to put object candidates into 3D. Kundu et al. [19] introduced the concept of CAD models to learn a low-dimensional shape space while extracting 2D region proposals. Another approach is to convert the front view representation, which can be done directly using existing LIDAR-based object detection methods. Wang et al. [20] performed depth estimation based on the front view to generate a pseudo-point cloud and used LIDAR-based target detection methods directly on the pseudo-point cloud. In contrast, Qian et al. [21] used a binocular camera to compute disparity for depth estimation, generating a pseudo-point cloud.

Recently, BEV-based object detection method [22] has achieved SOTA on the public dataset nuScenes. Converting the front view to BEV facilitates object detection and dramatically alleviates the occlusion problem of object detection in the front view perspective. However, the quality of BEV generation seriously affects the target detection performance. Currently, there are two ways to convert the front view to BEV: one is to use the internal and external parameters of the camera explicitly, and the other is to use the internal and external parameters implicitly. Mallot et al. [23] proposed IPM, which directly uses internal and external parameters to convert BEV, provided all objects are on the plane. However, bumps can seriously affect the quality of BEV generation and cause distortion. Although LSS [24] avoids the disadvantage of IPM, it uses depth prediction to generate BEV, while depth prediction needs strong prior knowledge. In order to obtain accurate depth information, Li et al. [26] proposed BEVDepth, which introduces LiDAR’s depth information to supervise the camera’s depth prediction in the training stage, and the obtained depth information has higher accuracy. There are also methods for generating BEV that implicitly utilize information external to the camera and do not require depth prediction. Lu et al. [27] generated BEV using MLP strategy and used a fixed matrix to transform the front view, do not depend on the input image. In contrast to MLP-based methods, BEV converting method proposed by Wang et al. [28] and Li et al. [29] is transformer-based and highly dependent on the input data.

2) *LiDAR-based 3D Object Detection*: The point cloud provided by LiDAR is a natural 3D space that provides accurate depth information. However, Due to the irregularity

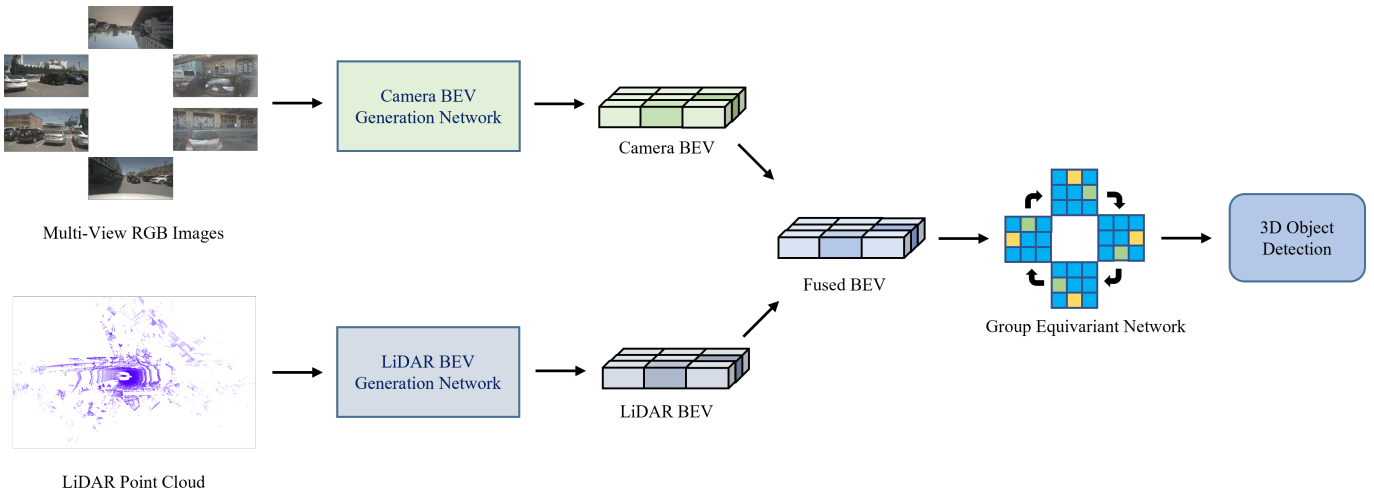


Fig. 1. The overall framework of the proposed GeqBevNet network. GeqBevNet first generates BEV through the camera BEV generation network and LiDAR BEV generation networks and fuses them. After fusing the BEV, the group equivariant network is embedded to extract the rotational equivariant features.

and disorder of point clouds, early work focused on directly processing raw point clouds. Qi et al. [30] proposed PointNet as the foundational work to process raw point clouds directly. The follow-up PointNet++ [31] made up for the deficiency that PointNet does not extract local features and improves the model’s generalization ability. Li et al. [32] defined an operation called  $\mathcal{X}$ -Conv, and regular convolution can process raw point clouds. However, the model’s input data is cumbersome if the point cloud is performed directly. To reduce the amount of data, Zhou et al. [33] processed the raw point cloud into regular voxels, which can be directly used for 3D convolution. Unlike voxels that divide into three dimensions, PointPillars proposed by Lang et al. [34] split the point cloud into 2D point cloud columns, which are then converted into BEV. This approach dramatically improves the speed of point cloud processing.

3) *Camera-LiDAR fusion for 3D Object Detection*: Since the single modality information provided by a single sensor is insufficient for 3D target detection in complex scenes, and the information provided by the camera and LiDAR are complementary in most scenes, most multi-sensor fusion efforts are based on cameras and LiDAR. Previous multi-sensor fusion works can be divided into two categories. One is camera-to-LiDAR. This work [11] used the image’s semantic features to enhance point clouds but lost semantic density. Another category is LiDAR-to-camera. This category of work project point clouds onto a 2D plane and then processes it using existing 2D object detection methods. Chen et al. [10] projected the point cloud into the front view, discarding the geometric features of the point cloud. In order to avoid the loss of semantic density or the loss of geometric features caused by fusion, the fusion of the camera and LiDAR in the same form becomes the focus of future fusion work. Recently, Liu et al. [15] proposed BEVFusion to fuse camera BEV with LiDAR BEV and achieved remarkable results in 3D object detection. However, Liang et al. [14] focused more on the robustness

of multi-sensor fusion in their BEV fusion work to study the perception performance of occlusion or single-sensor failure.

### B. Group Equivariant Network

In traditional convolutional neural networks(CNN), which have translational equivariant in convolution, the object processing of an image can not be affected by the object’s position in the image. However, it does not have the rotational equivariant. In previous work, rotational equivariant is usually obtained by simply rotating the training dataset images. Dillerman et al. [39] used rotational symmetry of images to predict the shape of early galaxies.

Group equivariant network is an equivariant network that uses group equivariant convolution to extract features with specific group properties. Cohen et al. [38] first proposed the group equivariant convolutional neural network, which lifted the traditional convolution to group with group properties. It was experimentally demonstrated that the group equivariant convolutional neural network has a higher degree of weight sharing and improves the network’s performance without significantly increasing the number of network parameters. Since larger groups require higher computational cost, Cohen et al. [40] proposed a related theoretical framework to address this issue to separate group size from computational cost. Finzi et al. [41] proposed a general group equivariant convolution called LieConv, which allows a flexible alternative to a given group. Hutchinson et al. [42] introduced self-attention to build a LieSelfAttention layer with group equivariant properties.

Despite the rapid progress in the study of group equivariant networks, it is still rarely used in 3D object detection or object recognition, and there are still significant challenges. Wang et al. [35] used equivariance as additional prior knowledge added to the network during continuous learning, which avoids an increase sharply in task increment caused by point cloud augmentation. Wu et al. [43] extract lightweight equivariant features on point clouds to improve real-time performance

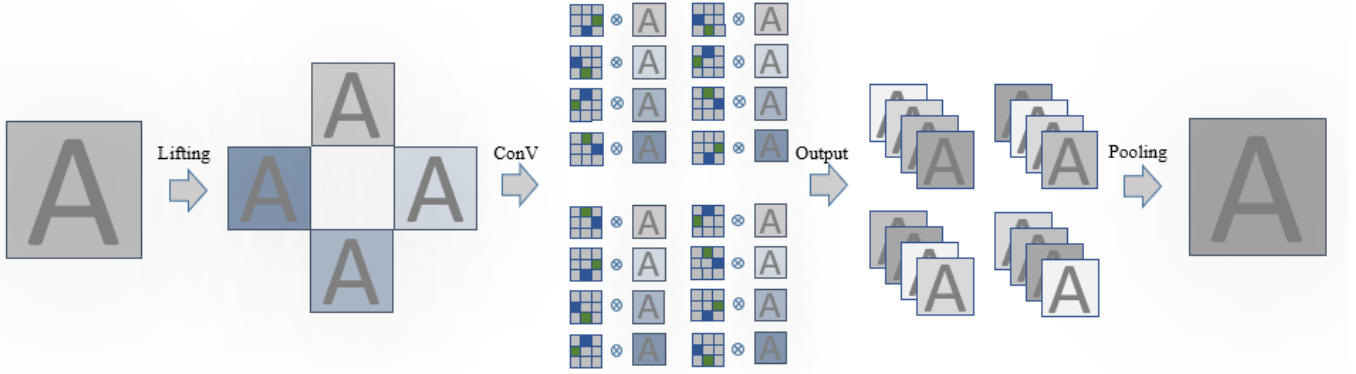


Fig. 2. Process of extracting rotational equivariant features with group equivariant network.

for 3D object detection. However, using rotational equivariant to solve the problems of 3d target detection on multi-sensor fusion target detection networks with rich data forms is still a challenge.

### III. PROPOSED METHOD

#### A. Preliminary

Mathematically, given that there are two domains,  $X$  and  $Y$ , both belonging to the group  $G$ , then the definition of equivariance can be expressed as:

$$I(g \cdot x) = g \cdot I(x) \quad (1)$$

where  $I$  is a function,  $g$  belongs to  $G$ ,  $x$  belongs to  $X$ , and  $g \cdot I(x)$  belongs to  $Y$ , and  $X \rightarrow Y$  is called an equivariant mapping, and both  $X$  and  $Y$  are homomorphisms in the group  $G$ . For traditional CNN, translational equivariant means that the result of translation followed by convolution of the target in the image is consistent with the translation. As defined by Cohen et al. [38], in traditional CNN, the definition of equivariance can be expressed as:

$$[L_g f](x) = f(g^{-1}x) \quad (2)$$

where  $L_g$  is a special group transform operator, and  $x$  is expressed as an image feature map.

Traditional CNN only has translational equivariant and cannot extract effective rotational orientation information. Previous work [38] proved that the traditional CNN does not have a rotational equivariant and proposed a related mathematical theory to enable CNN with a rotational equivariant. To achieve rotational equivariant for CNN, Cohen et al. [38] introduced the symmetry group  $p4$  and lifted the input image to the symmetry group  $p4$ , which is equivalent to extending the function and convolution kernel defined on the plane  $\mathbb{Z}^2$  to the symmetry group  $p4$ . They expressed this process mathematically as follows:

$$[f \star \psi](g) = \sum_{y \in \mathbb{Z}^2} \sum_k f_k(y) \psi_k(g^{-1}y) \quad (3)$$

The obtained image has specific properties of the symmetry group  $p4$  and the convolution operation is performed on the

symmetry group  $p4$ . This process can be defined by Cohen et al. [38] as follows:

$$[f \star \psi](g) = \sum_{h \in G} \sum_k f_k(h) \psi_k(g^{-1}h) \quad (4)$$

With the above processing, the image features acquire rotational equivariance while having translational equivariance.

#### B. BEV-level Equivariant Feature Extraction

In order to obtain the dense semantic information from the camera and the accurate geometric information from the LiDAR simultaneously, as shown in Fig. 1, we use BEV to unify the information from both modalities into the same form. In the camera BEV generation network, we encode the original surround view into BEV with LSS [24], where the depth prediction module predicts the depth with high reliability due to the strong prior. In addition, in the LiDAR BEV generation network, we use SECOND [46] as the backbone network for point cloud feature extraction. Therefore, compared with the faster Pointpillars [34], Voxels can retain more spatial information of point clouds.

After the image BEV and point cloud BEV are fused, we construct an embedded group equivariant network to extract the fused equivariant features. As shown in Fig. 2. The above fusion process can be expressed as:

$$F_{bev f} = f_{concat}(F_{bevi}(x), F_{bev p}(x)) \quad (5)$$

where  $F_{bevi}(x)$  denotes the image BEV features,  $F_{bev p}(x)$  denotes the point cloud BEV features and  $f_{concat}$  denotes the fusion BEV. Meanwhile, the constructed group equivariant network can be expressed as:

$$\begin{aligned} N_{geqbev} &= P(F_a[BN_{beveq}[GeqConV[F_{bev f}(x)]]) \\ &= P(F_g(x)) \end{aligned} \quad (6)$$

where  $GeqConV$  consists of BEV-level lifting layer and BEV group convolution layer,  $BN_{beveq}$  is the batch normalization that satisfies group  $G$ ,  $F_a$  is the activation function of the CNN,  $P$  denotes the pooling layer we construct and  $F_g(x)$  is the output of the activation function.

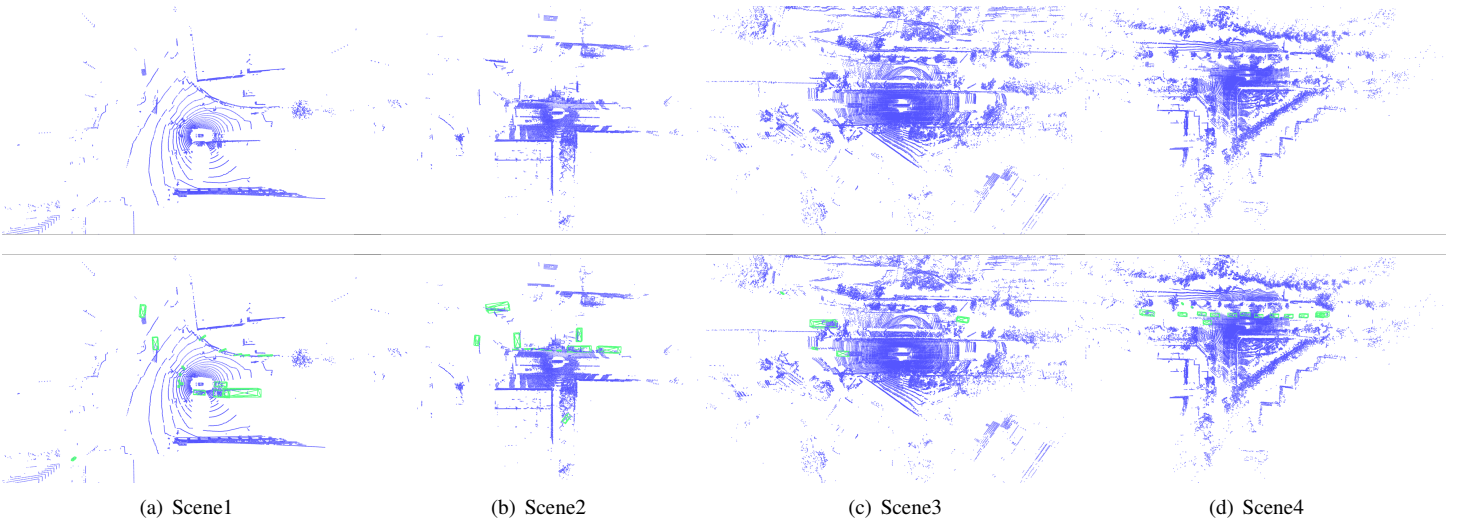


Fig. 3. 3D Object detection visualization performed by GeqBevNet.

Contrary to the traditional CNN, group equivariant convolutional neural networks require to lift features from plane  $\mathbb{Z}^2$  to group  $G$ . To satisfy this definition, according to (3), we construct a BEV-level lifting layer is called *BEVLift* and express as follows:

$$\begin{aligned}
 F_{bevlift} &= BEVLift(F_{bev}) \\
 &= [F_{bev} \star \psi](g) \\
 &= \sum_{n \in \mathbb{Z}^2} \sum_i F_{bevfi}(n) \psi_i(g^{-1}n)
 \end{aligned} \tag{7}$$

where  $F_{bev}$  is denotes the fused BEV feature map,  $\psi$  is the group convolution kernel with both translation and rotation properties,  $i$  is represents the number of channels and  $n$  belongs to plane  $\mathbb{Z}^2$ . Further, the BEV features initially on the plane  $\mathbb{Z}^2$  are lifted by one dimension after passing through the *BEVLift*. Therefore, the BEV features are lifted from  $(B, C, H, W)$  to  $(B, C, R, H, W)$ , and to satisfy the definition of convolution on the group, according to (4), we build the BEV group convolution as follows:

$$\begin{aligned}
 F_{geqconv} &= ConV_{beveq}(F_{bevlift}) \\
 &= [F_{bevlift} \star \psi](g) \\
 &= \sum_{m \in G} \sum_i F_{bevlifti}(m) \psi_i(g^{-1}m)
 \end{aligned} \tag{8}$$

where  $F_{bevlift}$  is the output of *BEVLift*, and  $m$  belongs to group  $g$ , we use the cycle group  $C4$  as the transform group with  $R$  in the shape of BEV as 4. After the *BEVLift* layer and the BEV group convolutional layer, we extract BEV-level rotational equivariant features from the BEV located in the plane  $\mathbb{Z}^2$ .

### C. BEV-level Equivariant Feature Pooling

Since the existing object detection head cannot directly detect objects and predict their orientation in the group, if we

modify the existing object detection head to satisfy the rotational equivariant feature, it cannot satisfy the embeddedness requirement of the group equivariant network we designed. Therefore, to address this issue, we degenerate it from the group to the plane  $\mathbb{Z}^2$ . The features on the group have both translational and rotational equivariance, while the traditional CNN only has translation equivariant. When the shape of the features on the group corresponds to the shape of the features on the plane  $\mathbb{Z}^2$ , we call it degenerating from the group to the plane  $\mathbb{Z}^2$ . We build the *BEVEqPooling* layer to eliminate the  $C4$  dimension, which can be expressed as:

$$F_{geqbev} = BEVEqPooling(F_g(x)) \tag{9}$$

By building the *BEVEqPooling* layer, we transfer the features from the group to the plane  $\mathbb{Z}^2$ , satisfying the requirements of embeddable group equivariant network.

## IV. EXPERIMENTS

To evaluate the performance of our proposed GeqBevNet, we conducted extensive experiments on the nuScenes dataset with different road scenes.

### A. Datasets

Since BEV generation requires a complete vehicle surround view, KITTI [44] only provides the front view. Waymo [45] has 5 cameras and lacks the camera information behind the vehicle, while nuScenes provides 6 complete vehicles surrounding information cameras and becomes the most popular public dataset for BEV generation. In addition to the 6 cameras, the nuScenes dataset is equipped with 32-line LiDAR and 5 millimeter-wave radars, and is equipped with an IMU.

Nuscenes dataset only selects key frames for labeling, and Boston and Singapore collected 40,000 key frames. A total of 23 classes of objects are labeled with 3D boxes, class information, and some important attributes. In terms of object

TABLE I  
COMPARISON WITH OTHER METHODS (MAP AND NDS) ON NUSCENES VALIDATION SET.

Method	Modality	Per-class										Metric	
		Car	Trunk	Bus	Trailer	C.V.	Ped.	Motor.	Bicycle	T.C.	Barrier	mAP $\uparrow$	NDS $\uparrow$
PointPillars [34]	L	78.7	37.2	49.7	26.2	6.56	61.2	20.2	0.85	18.9	41.4	34.1	49.9
FreeAnchor [9]	L	81.2	39.3	48.0	30.9	10.2	74.4	43.5	18.0	41.4	52.7	44.0	55.0
CenterPoint [25]	L	83.9	50.2	62.0	32.7	10.5	77.3	45.4	16.4	50.5	60.1	48.9	59.6
HotSpotNet [36]	L	84.0	56.2	67.4	38.0	20.7	82.6	66.2	49.7	65.8	64.3	59.5	66.0
PointPainting [11]	L+C	77.9	35.8	36.2	37.3	15.8	73.3	41.5	24.1	62.4	60.2	46.4	58.1
3D CVF [13]	L+C	83.0	45.0	48.8	<b>49.6</b>	15.9	74.2	51.2	30.4	62.9	65.9	52.7	62.3
MSF3DDETR [37]	L+C	<b>86.0</b>	58.0	<b>71.0</b>	40.0	21.0	83.0	67.0	<b>53.0</b>	67.0	61.0	60.7	66.7
GeqBevNet(ours)	L+C	85.6	<b>58.2</b>	70.8	39.0	<b>24.8</b>	<b>85.3</b>	<b>67.2</b>	51.8	<b>69.6</b>	<b>70.0</b>	<b>62.2</b>	<b>66.8</b>

Class names for class abbreviations: Construction Vehicle (C.V.), Pedestrian (Ped.), Traffic Cone (T.C.), Camera (C), LiDAR (L).

detection, it supports 10 types of object detection, such as cars, trucks, pedestrians, fences, etc.

In object detection, the following types of evaluation metrics are available: Average Precision (AP), Average Translation Error (ATE), Average Scale Error (ASE), Average Orientation Error (AOE), Average Velocity Error (AVE), and Average Attribute Error (AAE). In addition, the nuScenes dataset also proposes a nuScenes detection score (NDS), which is calculated using the six metrics mentioned above.

### B. Experimental Settings

We will focus on the three metrics of mAP, mAOE and NDS, and demonstrate the effectiveness of our network by comparing these three metrics with other advanced networks. We set the input image to  $1600 \times 900$ , and the point cloud range to  $[-54.0, -54.0, -5.0, 54.0, 54.0, 3.0]$ . In the training phase, in order to keep the iteration of the network stable, we added pre-trained weights, and then used the Tesla V100S to iterate the entire network for 6 epochs. The batch size of each epoch is set to 1, and the learning rate of the Adam optimizer is set to 0.001. In order to demonstrate the effectiveness of our constructed embedded group equivariant network, we did not use other data augmentation methods in our experiments.

### C. Results

In this section, we show the performance achieved on the nuScenes validation set and compare it with advanced object detection methods. We provide visualizations of 3D object detection results performed by GeqBevNet in different scenarios in Fig. 3. It shows that the GeqBevNet achieves promising performance in object orientation.

1) *Precision*: We compare the precision and NDS of our network with other advanced networks and place the results in Table I. GeqBevNet achieved promising results without using other data augmentation methods. We achieved 62.2% in mAP and 66.8% in NDS. Through the above results, we fully demonstrate the effectiveness of the embedded group equivariant network we constructed.

2) *Orientation*: Since group equivariant networks can extract more rotational equivariant features, to verify the performance of GeqBevNet in object orientation prediction, we evaluate the network’s AOE metrics for 9 classes and compare them with advanced networks. The results are shown in Table

II, in which Our network decreases to 0.325 on mAOE. And from Table II that the group equivariant network is more effective in predicting object orientation.

TABLE II  
COMPARISON WITH OTHER METHODS (AOE) ON NUSCENES VALIDATION SET.

Method	Modality	Metric
		mAOE $\downarrow$
DETR3D [16]	C	0.379
BEVFormer [29]	C	0.372
FreeAnchor [9]	L	0.530
PointPillars [34]	L	0.523
CenterPoint [25]	L	0.385
CenterFusion [4]	C+R	0.535
RCBEV4d [5]	C+R	0.445
BEVDepth [26]	L(S)+C	0.358
GeqBevNet(ours)	L+C	<b>0.325</b>

Radar(R),LiDAR Supervision(L(S)).

### D. Ablation

To demonstrate the effect of group equivariant network depth on the overall network, We conduct ablation experiments on the depth of group equivariant networks to obtain an optimal network depth.

From Section III, we know that the group equivariant network in GeqBevNet consists of *BEVLift* layer, BEV group convolutional layer, and *BEVEqPooling* layer. Among them, the *BEVLift* layer and *BEVEqPooling* layer do not require to increase or decrease the number of layers due to their particular functions, and we pay more attention to the BEV group convolutional layer, especially on its number of layers. We will choose the optimal number of layers  $N$  to obtain the best orientation prediction performance based on the lowest mAOE of the network.

We set up the group equivariant network with different depths in GeqBevNet and conducted experiments to obtain the results shown in Table III. We can observe that when  $N = 3$ , the network achieves the best results on mAOE. After  $N = 3$ , mAOE gradually increases. According to the ablation experiments, the depth of the group equivariant network does not mean that extracting deeper rotational equivariant features can improve the network’s orientation prediction performance. In addition, there may be insufficient feature extraction for

TABLE III  
RESULTS OF GROUP EQUIVARIANT NETWORKS WITH DIFFERENT NETWORK DEPTHS ON NUSCENES VALIDATION SET.

Network Depth	Per-class									Metric
	Car	Trunk	Bus	Trailer	C.V.	Ped.	Motor.	Bicycle	Barrier	mAOE↓
2	0.121	0.118	0.096	0.598	0.973	0.387	<b>0.247</b>	0.466	0.116	0.347
3	<b>0.119</b>	<b>0.105</b>	<b>0.071</b>	<b>0.537</b>	<b>0.914</b>	0.384	0.286	<b>0.394</b>	<b>0.112</b>	<b>0.325</b>
4	0.120	0.130	0.133	0.733	0.984	<b>0.376</b>	0.299	0.459	0.130	0.374

TABLE IV  
COMPARISON RESULTS OF DIFFERENT POOLING METHODS ON NUSCENES VALIDATION SET.

Pooling Methods	Per-class									Metric
	Car	Trunk	Bus	Trailer	C.V.	Ped.	Motor.	Bicycle	Barrier	mAOE↓
Max Pooling	0.247	0.309	0.411	0.902	1.028	0.775	0.642	0.984	0.336	0.626
Average Pooling	<b>0.112</b>	0.110	0.078	0.593	<b>0.898</b>	<b>0.370</b>	<b>0.266</b>	0.490	0.115	0.337
BevEq Pooling	0.119	<b>0.105</b>	<b>0.071</b>	<b>0.537</b>	0.914	0.384	0.286	<b>0.394</b>	<b>0.112</b>	<b>0.325</b>

shallow rotational equivariant features, which still cannot improve the average orientation error of the object.

Further, in order to prove the effectiveness of our constructed *BEVEqPooling* layer, we conducted ablation experiments with average pooling and max pooling, and the obtained results are shown in Table IV. We can observe that our built *BEVEqPooling* layer is effective in decreasing the AOE of the network compared to the average pooling and max pooling.

## V. CONCLUSION

In this paper, we propose GeqBevNet, in which a group equivariant network is embedded into the object detection network to address the perturbations of 3D objects under different driving conditions. The group equivariant network enables the extraction of BEV-level rotational equivariant features to obtain better performance in object detection tasks. In addition, the proposed group equivariant network can be easily embedded into other end-to-end networks to increase their orientation prediction performance.

Since the rotation of the actual road scene may be more sophisticated, there are many rotation factors that we may have not considered. Currently, we only consider the issue of large-scale scene rotation. In the future, we will continue to explore the existing problems and extend the group equivariant network to more complex and applicable specific discrete groups, focusing on the issues caused by road scene rotation.

## ACKNOWLEDGMENT

This research is supported by the National Natural Science Foundation of China (No.42130112) and KartoBit Research Network(No.KRN2201CA). Partially supported by ‘Fujian Science & Technology Innovation Laboratory for Optoelectronic Information of China’ (No.2021ZZ120). The authors would like to thank Xihao Wang and Jiaming Lei for their helpful discussion.

## REFERENCES

- [1] Badue C, Guidolini R, Carneiro R V, et al. Self-driving cars: A survey[J]. Expert Systems with Applications, 2021, 165: 113816.
- [2] Panchpor A A, Shue S, Conrad J M. A survey of methods for mobile robot localization and mapping in dynamic indoor environments[C]//2018 Conference on Signal Processing And Communication Engineering Systems (SPACES). IEEE, 2018: 138-144.
- [3] Wang X, Lei J, Lan H, et al. DuEqNet: Dual-Equivariance Network in Outdoor 3D Object Detection for Autonomous Driving[J]. arXiv preprint arXiv:2302.13577, 2023.
- [4] Nabati R, Qi H. Centerfusion: Center-based radar and camera fusion for 3d object detection[C]//Proceedings of the IEEE/CVF Winter Conference on Applications of Computer Vision. 2021: 1527-1536.
- [5] Zhou T, Chen J, Shi Y, et al. Bridging the view disparity between radar and camera features for multi-modal fusion 3d object detection[J]. IEEE Transactions on Intelligent Vehicles, 2023, 8(2): 1523-1535.
- [6] Wang Y, Wei X, Tang X, et al. Adaptive fusion cnn features for rgbt object tracking[J]. IEEE Transactions on Intelligent Transportation Systems, 2021, 23(7): 7831-7840.
- [7] Herman S, Ismail K. Single Camera Object Detection for Self-Driving Vehicle: A Review[J]. Journal of the Society of Automotive Engineers Malaysia, 2017, 1(3): 198-207.
- [8] Qian K, Zhu S, Zhang X, et al. Robust multimodal vehicle detection in foggy weather using complementary lidar and radar signals[C]//Proceedings of the IEEE/CVF Conference on Computer Vision and Pattern Recognition. 2021: 444-453.
- [9] Zhang X, Wan F, Liu C, et al. Freeanchor: Learning to match anchors for visual object detection[J]. Advances in neural information processing systems, 2019, 32.
- [10] Chen X, Ma H, Wan J, et al. Multi-view 3d object detection network for autonomous driving[C]//Proceedings of the IEEE conference on Computer Vision and Pattern Recognition. 2017: 1907-1915.
- [11] Vora S, Lang A H, Helou B, et al. Pointpainting: Sequential fusion for 3d object detection[C]//Proceedings of the IEEE/CVF conference on computer vision and pattern recognition. 2020: 4604-4612.
- [12] Li C, Wei X, Yu H, et al. An enhanced squeezeNet based network for real-time road-object segmentation[C]//2019 IEEE Symposium Series on Computational Intelligence (SSCI). IEEE, 2019: 1214-1218.
- [13] Yoo J H, Kim Y, Kim J, et al. 3d-cvf: Generating joint camera and lidar features using cross-view spatial feature fusion for 3d object detection[C]//Computer Vision—ECCV 2020: 16th European Conference, Glasgow, UK, August 23–28, 2020, Proceedings, Part XXVII 16. Springer International Publishing, 2020: 720-736.
- [14] Liang T, Xie H, Yu K, et al. Bevfusion: A simple and robust lidar-camera fusion framework[J]. arXiv preprint arXiv:2205.13790, 2022.
- [15] Liu Z, Tang H, Amini A, et al. BEVFusion: Multi-Task Multi-Sensor Fusion with Unified Bird’s-Eye View Representation[J]. arXiv preprint arXiv:2205.13542, 2022.
- [16] Wang Y, Guizilini V C, Zhang T, et al. Detr3d: 3d object detection from multi-view images via 3d-to-2d queries[C]//Conference on Robot Learning. PMLR, 2022: 180-191.
- [17] Caesar H, Bankiti V, Lang A H, et al. nuscenes: A multimodal dataset for autonomous driving[C]//Proceedings of the IEEE/CVF conference on computer vision and pattern recognition. 2020: 11621-11631.

- [18] Chen X, Kundu K, Zhang Z, et al. Monocular 3d object detection for autonomous driving[C]//Proceedings of the IEEE conference on computer vision and pattern recognition. 2016: 2147-2156.
- [19] Kundu A, Li Y, Rehg J M. 3d-rcnn: Instance-level 3d object reconstruction via render-and-compare[C]//Proceedings of the IEEE conference on computer vision and pattern recognition. 2018: 3559-3568.
- [20] Wang Y, Chao W L, Garg D, et al. Pseudo-lidar from visual depth estimation: Bridging the gap in 3d object detection for autonomous driving[C]//Proceedings of the IEEE/CVF Conference on Computer Vision and Pattern Recognition. 2019: 8445-8453.
- [21] Qian R, Garg D, Wang Y, et al. End-to-end pseudo-lidar for image-based 3d object detection[C]//Proceedings of the IEEE/CVF Conference on Computer Vision and Pattern Recognition. 2020: 5881-5890.
- [22] Huang J, Huang G. BEVPoolv2: A Cutting-edge Implementation of BEVDet Toward Deployment[J]. arXiv preprint arXiv:2211.17111, 2022.
- [23] Mallot H A, Bühlhoff H H, Little J J, et al. Inverse perspective mapping simplifies optical flow computation and obstacle detection[J]. *Biological cybernetics*, 1991, 64(3): 177-185.
- [24] Philion J, Fidler S. Lift, splat, shoot: Encoding images from arbitrary camera rigs by implicitly unprojecting to 3d[C]//Computer Vision—ECCV 2020: 16th European Conference, Glasgow, UK, August 23–28, 2020, Proceedings, Part XIV 16. Springer International Publishing, 2020: 194-210.
- [25] Yin T, Zhou X, Krahenbuhl P. Center-based 3d object detection and tracking[C]//Proceedings of the IEEE/CVF conference on computer vision and pattern recognition. 2021: 11784-11793.
- [26] Li Y, Ge Z, Yu G, et al. Bevdepth: Acquisition of reliable depth for multi-view 3d object detection[J]. arXiv preprint arXiv:2206.10092, 2022.
- [27] Lu C, van de Molengraft M J G, Dubbelman G. Monocular semantic occupancy grid mapping with convolutional variational encoder–decoder networks[J]. *IEEE Robotics and Automation Letters*, 2019, 4(2): 445-452.
- [28] Wang Y, Guizilini V C, Zhang T, et al. Detr3d: 3d object detection from multi-view images via 3d-to-2d queries[C]//Conference on Robot Learning. PMLR, 2022: 180-191.
- [29] Li Z, Wang W, Li H, et al. Bevformer: Learning bird’s-eye-view representation from multi-camera images via spatiotemporal transformers[C]//Computer Vision—ECCV 2022: 17th European Conference, Tel Aviv, Israel, October 23–27, 2022, Proceedings, Part IX. Cham: Springer Nature Switzerland, 2022: 1-18.
- [30] Qi C R, Su H, Mo K, et al. Pointnet: Deep learning on point sets for 3d classification and segmentation[C]//Proceedings of the IEEE conference on computer vision and pattern recognition. 2017: 652-660.
- [31] Qi C R, Yi L, Su H, et al. Pointnet++: Deep hierarchical feature learning on point sets in a metric space[J]. *Advances in neural information processing systems*, 2017, 30.
- [32] Li Y, Bu R, Sun M, et al. Pointcnn: Convolution on x-transformed points[J]. *Advances in neural information processing systems*, 2018, 31.
- [33] Zhou Y, Tuzel O. Voxelnet: End-to-end learning for point cloud based 3d object detection[C]//Proceedings of the IEEE conference on computer vision and pattern recognition. 2018: 4490-4499.
- [34] Lang A H, Vora S, Caesar H, et al. Pointpillars: Fast encoders for object detection from point clouds[C]//Proceedings of the IEEE/CVF conference on computer vision and pattern recognition. 2019: 12697-12705.
- [35] Wang X, Wei X. Continual Learning for Pose-Agnostic Object Recognition in 3D Point Clouds[J]. arXiv preprint arXiv:2209.04840, 2022.
- [36] Chen Q, Sun L, Wang Z, et al. Object as hotspots: An anchor-free 3d object detection approach via firing of hotspots[C]//Computer Vision—ECCV 2020: 16th European Conference, Glasgow, UK, August 23–28, 2020, Proceedings, Part XXI 16. Springer International Publishing, 2020: 68-84.
- [37] Erabati G K, Araujo H. MSF3DDETR: Multi-Sensor Fusion 3D Detection Transformer for Autonomous Driving[J]. arXiv preprint arXiv:2210.15316, 2022.
- [38] Cohen T, Welling M. Group equivariant convolutional networks[C]//International conference on machine learning. PMLR, 2016: 2990-2999.
- [39] Dieleman S, De Fauw J, Kavukcuoglu K. Exploiting cyclic symmetry in convolutional neural networks[C]//International conference on machine learning. PMLR, 2016: 1889-1898.
- [40] Cohen T S, Welling M. Steerable cnns[J]. arXiv preprint arXiv:1612.08498, 2016.
- [41] Finzi M, Stanton S, Izmailov P, et al. Generalizing convolutional neural networks for equivariance to lie groups on arbitrary continuous data[C]//International Conference on Machine Learning. PMLR, 2020: 3165-3176.
- [42] Hutchinson M J, Le Lan C, Zaidi S, et al. Lietransformer: Equivariant self-attention for lie groups[C]//International Conference on Machine Learning. PMLR, 2021: 4533-4543.
- [43] Wu H, Wen C, Li W, et al. Transformation-Equivariant 3D Object Detection for Autonomous Driving[J]. arXiv preprint arXiv:2211.11962, 2022.
- [44] Geiger A, Lenz P, Urtasun R. Are we ready for autonomous driving? the kitti vision benchmark suite[C]//2012 IEEE conference on computer vision and pattern recognition. IEEE, 2012: 3354-3361.
- [45] Sun P, Kretschmar H, Dotiwalla X, et al. Scalability in perception for autonomous driving: Waymo open dataset[C]//Proceedings of the IEEE/CVF conference on computer vision and pattern recognition. 2020: 2446-2454.
- [46] Yan Y, Mao Y, Li B. Second: Sparsely embedded convolutional detection[J]. *Sensors*, 2018, 18(10): 3337.